

## Separation of a benzene and nitric oxide mixture by a molecule prism

Bum Suk Zhao, Sung Hyup Lee, Hoi Sung Chung, Sungu Hwang, Wee Kyung Kang, Bretislav Friedrich, and Doo Soo Chung

Citation: *The Journal of Chemical Physics* **119**, 8905 (2003); doi: 10.1063/1.1613934

View online: <http://dx.doi.org/10.1063/1.1613934>

View Table of Contents: <http://scitation.aip.org/content/aip/journal/jcp/119/17?ver=pdfcov>

Published by the [AIP Publishing](#)

---

### Articles you may be interested in

[Optical chromatographic sample separation of hydrodynamically focused mixtures](#)

*Biomicrofluidics* **8**, 064102 (2014); 10.1063/1.4901824

[Molecular dynamics simulations of transport and separation of carbon dioxide–alkane mixtures in carbon nanopores](#)

*J. Chem. Phys.* **120**, 8172 (2004); 10.1063/1.1688313

[Revealing the physicochemical mechanism for ultrasonic separation of alcohol–water mixtures](#)

*J. Chem. Phys.* **117**, 3874 (2002); 10.1063/1.1495849

[Molecular lens applied to benzene and carbon disulfide molecular beams](#)

*J. Chem. Phys.* **114**, 8293 (2001); 10.1063/1.1367380

[Nonequilibrium molecular dynamics simulation of transport and separation of gases in carbon nanopores. II. Binary and ternary mixtures and comparison with the experimental data](#)

*J. Chem. Phys.* **112**, 910 (2000); 10.1063/1.480618

---



# Separation of a benzene and nitric oxide mixture by a molecule prism

Bum Suk Zhao, Sung Hyup Lee, Hoi Sung Chung, and Sungu Hwang<sup>a)</sup>

*School of Chemistry, Seoul National University, Seoul 151-747, Korea*

Wee Kyung Kang

*Department of Chemistry, Soongsil University, Seoul 156-743, Korea*

Bretislav Friedrich

*Department of Chemistry and Chemical Biology, Harvard University, Cambridge, Massachusetts 02138*

Doo Soo Chung<sup>b)</sup>

*School of Chemistry, Seoul National University, Seoul 151-747, Korea*

(Received 9 June 2003; accepted 7 August 2003)

In molecule optics, a matter wave of molecules is manipulated by a molecule-optical component made out of external, typically radiative, fields. The molecule-optical index of refraction,  $n$ , for a nonresonant IR laser pulse focused onto a molecular beam can be obtained from the energy conservation and wave properties of molecules. Experimentally measured values of  $n$  for benzene and nitric oxide agreed well with the calculated values. Since  $n$  depends on the properties of molecules as well as those of the laser field, a molecule prism composed of the focused nonresonant laser field can separate a multi-component molecular beam into several components according to their molecule-optical refractive indices  $n$ . We obtained a chromatographic resolution of 0.62 for the spatial separation of a mixture beam of benzene and nitric oxide using a focused Nd:YAG laser pulse as a molecule prism. © 2003 American Institute of Physics. [DOI: 10.1063/1.1613934]

## I. INTRODUCTION

Significant progress in the manipulation of atoms via light forces has opened up a new field of atom optics and a number of atom-optical components have been proposed and demonstrated. Examples include an atom lens,<sup>1</sup> an interferometer,<sup>2</sup> a grating,<sup>2</sup> and a mirror.<sup>3</sup> Molecule optics is a natural extension of atom optics. Since most substances in nature are molecules rather than atoms, the development of molecule optics holds the promise of becoming another important cornerstone in the control of matter. Practical applications of molecule optics would contribute to the development of areas such as nano-lithography, molecular electronics and molecular engineering, to name but a few. Molecule-optical components based on light forces, however, cannot be realized by the same mechanisms as in atom optics since the complex vibrational and rotational structures of molecules prevent them from possessing cycling transitions.<sup>4</sup>

When atoms or molecules are placed in a nonresonant laser field, the nonresonant dipole force resulting from the interaction between the induced dipoles and the laser electric field can be exerted on the atoms or molecules regardless of their internal structures. Along with the numerous and discerning theoretical suggestions,<sup>5</sup> a limited number of experiments on the deflection of molecular beams,<sup>6</sup> molecular alignment,<sup>7</sup> rotational acceleration of molecules,<sup>8</sup> and a thin standing wave grating<sup>9</sup> have been reported. Recently, mol-

ecule lenses were realized and the characteristic lens parameters were determined.<sup>10,11</sup> These molecule lenses had an aberration similar to optical lenses' chromatic aberration. Then the part of a molecule lens with a large aberration can be regarded as a molecule prism, which disperses the components of a molecular beam with different de Broglie wavelengths according to the molecule-optical analog of the index of refraction in photon optics. As the next step on the way towards the realization of molecule optics, we investigate the properties of a molecule prism. We develop a theory of the prism based on the nonresonant dipole force and demonstrate its properties experimentally by spatially separating the components of a mixed neutral molecular beam of benzene and nitric oxide. Unlike laser cooling of atoms or molecules, an optical separation technique using the molecule prism requires manipulation of only one translational degree of freedom of the molecular motion. Thus the mixture of molecules could be separated via a much simpler scheme than that required for cooling.

## II. MOLECULE-OPTICAL REFRACTIVE INDEX

The molecule-optical refractive index is a mirror image of the refractive index for light, with the roles of molecules and photons interchanged. A focused laser beam is equivalent to a molecule prism, which disperses the mixture beam of molecules having different molecule-optical refractive indices. In analogy to the photon-optical refractive index, the molecule-optical index of refraction for a matter wave of molecules with mass  $m$  traveling through an external field with a potential  $V(\mathbf{r})$  at  $\mathbf{r}$  can be defined as<sup>12</sup>

$$n(\mathbf{r}) = k(\mathbf{r})/k_0, \quad (1)$$

<sup>a)</sup>Present address: School of Free Major, Miryang National University, Gyeongnam 627-702, Korea.

<sup>b)</sup>Author to whom correspondence should be addressed. Electronic mail: dschung@snu.ac.kr

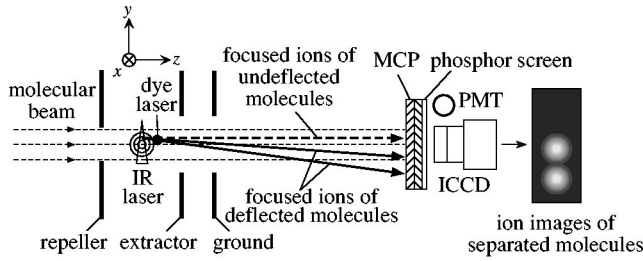


FIG. 1. Schematics of the setup for a molecule prism. The molecular beam propagates along the  $z$  axis and the laser beam along the  $x$  axis. The nonresonant dipole force is exerted along the  $y$  axis. After deflection, molecules are ionized by a dye laser pulse and focused onto a detector. The image of molecular ions on the phosphor screen is detected by PMT or ICCD camera.

where  $k(\mathbf{r})$  and  $k_0$  are the wavevectors of the molecular wave in the field and in the field-free region, respectively. In a nonresonant field, the energy conservation law requires that

$$E_0 = \frac{(\hbar k_0)^2}{2m} = \frac{(\hbar k)^2}{2m} + V(\mathbf{r}) = E(\mathbf{r}), \quad (2)$$

where  $E(\mathbf{r})$  and  $E_0$  are respectively the total energy in the field and in the field-free region. Since the corresponding group velocities of the molecules are given by

$$v_0^g = \frac{dE_0}{\hbar dk_0} \quad \text{and} \quad v^g = \frac{dE}{\hbar dk}, \quad (3)$$

we see that

$$n(\mathbf{r}) = \frac{v^g}{v_0^g} = \left(1 - \frac{V(\mathbf{r})}{E}\right)^{1/2}. \quad (4)$$

Hence  $n(\mathbf{r}) > 1$  for an attractive potential,  $V(\mathbf{r}) < 0$ , and  $n(\mathbf{r}) < 1$  for a repulsive potential,  $V(\mathbf{r}) > 0$ . In the weak-field limit the potential due to the interaction of a nonresonant laser field and the induced dipole of a molecule takes the form<sup>3</sup>

$$V(\mathbf{r}) = -\alpha \eta_0 I(\mathbf{r})/2, \quad (5)$$

where  $I(\mathbf{r})$  is the laser intensity,  $\alpha$  the mean static molecular polarizability, and  $\eta_0$  the vacuum impedance. Then

$$n(r) = \sqrt{1 + (\alpha \eta_0 I(\mathbf{r})/2mv_0^2)}, \quad (6)$$

where  $v_0$  is the group velocity of a molecular wave along the  $z$  axis (see Fig. 1). Let us consider a molecular beam propagating along the  $z$  axis at a velocity  $v_0$ , which is crossed by a Gaussian laser pulse near  $x=0$ ,  $I(y, z, t) = I_0 \exp[-2(y^2 + z^2)/w_0^2] \exp[-4(\ln 2)t^2/\tau^2]$ , where  $w_0$ ,  $I_0$ , and  $\tau$  denote the waist radius, peak intensity, and pulse width, respectively. This Gaussian pulse is then equivalent to a graded-index molecule lens with the molecule-optical refractive index

$$n(y, z, t) \approx 1 + \frac{\alpha \eta_0 I_0}{2mv_0^2} \exp[-2(y^2 + z^2)/w_0^2] \times \exp[-4(\ln 2)t^2/\tau^2]. \quad (7)$$

Fermat's principle in optics leads to a differential equation for the propagation of light rays through a medium characterized by a refractive index. For molecular rays propagating

nearly along the  $z$  axis in the  $yz$  plane, Fermat's principle can be simplified to the form (paraxial approximation)

$$\frac{d^2 y}{dz^2} \approx \frac{d \ln n}{dy}. \quad (8)$$

By setting  $z = v_0 t$  and integrating Eq. (8) over  $t$ , the velocity component imparted in the  $y$ -direction,  $\Delta v_y$  of a molecular ray passing through  $y = y_0$ , is given by

$$\Delta v_y = -\frac{\alpha \eta_0 I_0 y_0}{mv_0 w_0} \times \exp(-2y_0^2/w_0^2) \sqrt{\frac{2\pi}{1 + 2 \ln 2 [w_0/(v_0 \tau)]^2}}, \quad (9)$$

which leads to a deflection angle

$$\theta \approx \Delta v_y / v_0. \quad (10)$$

Note that the result for  $\Delta v_y$  in Eq. (9) is the same as the previous results derived from Newton's second law.<sup>10,11</sup>

The interaction of a molecular beam with a Gaussian laser field has properties similar to those of a SELFOC slab,<sup>13</sup> which is the trade name for a dielectric slab having a parabolic refractive index profile. Based on Eq. (7), we can define the refractive index along the  $y$  axis:

$$n(y) = 1 + \frac{\alpha \eta_0 I_0}{2mv_0^2} \exp(-2y^2/w_0^2). \quad (11)$$

For small  $y$ ,  $n(y)$  becomes parabolic:

$$n(y) \approx n_0 \left(1 - \frac{Ay^2}{2}\right), \quad (12)$$

with

$$n_0 = 1 + \alpha \eta_0 I_0 / 2mv_0^2 \quad \text{and} \quad A = 2\alpha \eta_0 I_0 / mv_0^2 w_0^2. \quad (13)$$

The focal length of a thin SELFOC slab of thickness  $L$  having a graded-index profile of Eq. (13) is given by

$$f \approx \frac{1}{n_0 \sqrt{A} \sin(L\sqrt{A})} \approx \frac{w_0^2}{4(n_0 - 1)L}. \quad (14)$$

Then choosing the thickness of the equivalent molecule-optical SELFOC slab as

$$L = \frac{w_0}{2} \sqrt{\frac{2\pi}{1 + 2 \ln 2 [w_0/(v_0 \tau)]^2}}, \quad (15)$$

the slab's focal length becomes identical to that derived from Newton's second law.<sup>10,11</sup> The maximum deflection is imparted for a molecular ray passing through the portion of the SELFOC slab near  $y = \pm w_0/2$  and leads to a deflection angle

$$\theta_{\max} \approx -\frac{\alpha \eta_0 I_0}{2\sqrt{e}mv_0^2} \sqrt{\frac{2\pi}{1 + 2 \ln 2 [w_0/(v_0 \tau)]^2}} = -\frac{L(n_0 - 1)}{\sqrt{e}w_0}. \quad (16)$$

As a consequence of the purely attractive nature of the induced dipole potential, the deflection angle is negative for

positive  $y$  and vice versa. Note that the deflection angle in Eq. (16) is equivalent to the deviation angle of a thin prism having an apex angle of  $L/(\sqrt{\epsilon}w_0)$ . Therefore, the portion near  $y = \pm w_0/2$  of the SELFOC slab acts as a molecule prism made up of a nonresonant laser field that separates molecular species as an optical prism disperses light of different colors.

### III. EXPERIMENT

The optical separation instrument, similar to the previous one,<sup>11</sup> consists of two parts, a molecule prism and a time-of-flight mass spectrometer (TOFMS) with a two-dimensional imaging detector (Fig. 1). A neutral molecular beam is formed by expanding a mixture of 50 torr benzene and 70 torr nitric oxide mixed with argon to a total pressure of 2 atm at a rate of 10 Hz. A circularly polarized 1064-nm Nd:YAG laser pulse of 7 ns duration ( $\tau$ ) and  $15.5 \mu\text{m}$  waist radius ( $w_0$ ) is focused into the pulsed molecular beam and acts as a molecule prism. The center of laser focus, the directions of propagation of the laser and the molecular beam are chosen as the origin,  $x$  axis, and  $z$  axis, respectively. The molecular rays deflected by the molecule prism are then crossed by a dye laser pulse, which ionizes molecules through multiphoton-ionization processes. The dye laser is pumped by the second harmonics of another Nd:YAG laser and adjusted to generate pulses of 644.1 nm wavelength, 5 ns pulse width, and 2 mJ/pulse energy. At 644.1 nm, benzene and nitric oxide are ionized via a multiphoton-ionization process and a resonance-enhanced-multiphoton-ionization process,  $1^1\Sigma^+(v=1) \leftarrow 2^2\Sigma^+(v=1) \leftarrow 2^2\Pi$ , respectively.<sup>14</sup> Note that the velocity changes from the remaining energies during the chosen ionization processes at 644.1 nm are negligible and the velocity of a molecular ion is the same as that of the parent neutral molecule;  $\mathbf{v}(\text{neutral molecule}) \approx \mathbf{v}(\text{molecular ion})$ . The resultant molecular ions are then accelerated and focused by three electrodes, a repeller, an extractor, and a ground, onto the front of a microchannel plate (MCP) after flying 127 cm through a TOF tube. These electrodes perform velocity map imaging by maintaining the ratio of the repeller voltage  $V_R$  to the extractor voltage  $V_E$ ,<sup>15</sup> which ratio is about 1.55 in our setup. During the traveling time of molecular ions ( $=\text{TOF}$ ), unaccelerated neutral molecules proceed a distance of  $\text{TOF} \times v_0(\text{neutral molecule})$  along the  $z$  axis with the same  $y$  shift as molecular ions ( $\Delta Y$ ). In order to investigate the spatial separation of neutral molecules, the focusing electrode voltages are adjusted alternatively as  $V_R = 1500 \text{ V}$  and  $V_E = 970 \text{ V}$  for benzene and  $V_R = 580 \text{ V}$  and  $V_E = 375 \text{ V}$  for nitric oxide, which values yield the same TOFs for the chosen species for each acquisition cycle. Ion signals amplified by the MCP hit a phosphor screen at the back of the MCP to result in luminescence, which is detected by a photomultiplier tube (PMT) and an intensified charge coupled device (ICCD) camera. To obtain the images of the selected species only, TTL signals are applied to gate the intensifier of the ICCD.

The trajectories of neutral molecules are deduced from the two-dimensional images of molecular ions on the ICCD. The velocity change of the deflected and then ionized mol-

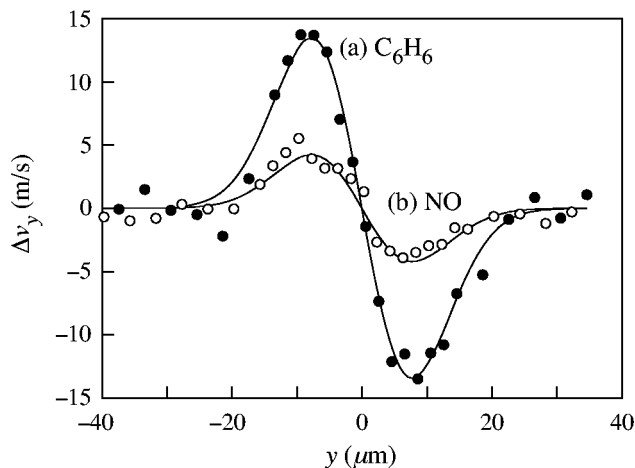


FIG. 2. The deflection velocity changes of (a) benzene (closed circles) and (b) nitric oxide (open circles) along the  $y$  axis are plotted as a function of the relative position of the IR laser focus from the dye laser focus. The IR laser is circularly polarized with peak intensity  $I_0 = 2.0 \times 10^{12} \text{ W/cm}^2$ . The solid curves show the fitting results from which  $w_0$  and  $n_0$  are obtained. The waist radius of the deflecting laser  $w_0 = 15.5 \mu\text{m}$  is determined from the benzene data.

ecule is determined from the image shift  $\Delta Y (= Y_{\text{ON}} - Y_{\text{OFF}}$ , where  $Y_{\text{ON}}$  and  $Y_{\text{OFF}}$  are the  $y$  coordinates of molecular ions at the MCP with the deflecting laser on and off, respectively) and the TOF of the ionized molecule:

$$\Delta v_y = \frac{\Delta Y}{\text{TOF}}. \quad (17)$$

Since the velocities along the  $y$  axis of a molecular ion and the parent neutral molecule are almost equal, the  $y$  coordinate of the neutral molecule, which has an initial velocity  $v_0 \hat{z}$  and has passed through the molecule prism at ( $y = y_0, z = 0; t = 0$ ), is the same as the molecular ion's  $y$  coordinate  $y_0 + \Delta Y$ . On the other hand, the change in velocity along the  $z$  axis,  $\Delta v_z$ , is negligible since  $v_0 \gg \Delta v_z$ . The position of neutral molecules, therefore, can be represented by the  $y$ - $z$  coordinate

$$(y_0 + \Delta Y, v_0 \times \text{TOF}; t = \text{TOF}). \quad (18)$$

### IV. RESULTS AND DISCUSSION

The molecule-optical refractive indices are deduced from the deflections of the molecular species measured as a function of  $y_0$  using Eqs. (7) and (9) as described in the previous reports.<sup>10,11</sup> Figure 2 shows the velocity changes of (a) benzene and (b) nitric oxide molecules and a fit of experimental data (circles) to Eq. (9). The value of  $15.5 \mu\text{m}$  for  $w_0$ , the waist radius of the deflecting laser, is determined from the benzene data which provide larger image shifts than nitric oxide. The data for nitric oxide yield the same waist radius values as the benzene data with a larger uncertainty. The fixed value of  $w_0 = 15.5 \mu\text{m}$  is then used for fitting the nitric oxide data. The maximum molecule-optical refractive indices  $n_0$  with the laser peak intensity  $I_0 = 2.0 \times 10^{12} \text{ W/cm}^2$  are 1.070 and 1.022 for benzene and nitric oxide, respectively. The  $n_0$  values can also be calculated from Eq. (13). Average static polarizabilities<sup>16</sup> of benzene



$10.3 \times 10^{-24} \text{ cm}^3$  and nitric oxide  $1.7 \times 10^{-24} \text{ cm}^3$  give  $n_0(\text{benzene})_{\text{cal}} = 1.098$  and  $n_0(\text{nitric oxide})_{\text{cal}} = 1.042$ . The uncertainty ranges of  $n_0 - 1$  and  $n_{0,\text{cal}} - 1$  values are about 20% and 30%, respectively. Experimental uncertainties can stem from the measurement of the laser pulse energy, pulse width, waist radius, molecular velocity  $v_0$  in the field-free region, and average static polarizabilities. For benzene, the  $n_0$  value obtained from fitting agrees well with the  $n_{0,\text{cal}}$  value while the agreement is somewhat less for nitric oxide. These analyses are based on the assumption that the multi-longitudinal mode spikes of our deflection laser prohibit the molecules from aligning along the plane of circular polarization. If the molecules are aligned along the plane perfectly, the effective molecular polarizability values become  $\alpha_{\perp}$  for the oblate benzene and  $(\alpha_{\parallel} + \alpha_{\perp})/2$  for the linear nitric oxide. Since the ratios  $\alpha_{\parallel}/\alpha_{\perp}$  are approximately 0.5 for benzene and 2 for nitric oxide, increment factors of the perfectly aligned molecular polarizability to the average static polarizability  $(\alpha_{\parallel} + 2\alpha_{\perp})/3$  are 6/5 for benzene and 9/8 for nitric oxide. Then the waist radius obtained from the fit using Eq. (9) can be underestimated since molecules passing through near the center ( $y=0$ ) will be deflected more due to the increased effective molecular polarizability. Since  $n_0 - 1$  and  $n_{0,\text{cal}} - 1$  are approximately proportional to  $w_0^2$  and  $1/w_0^2$ , respectively, a 10% underestimation of  $w_0$  decreases the  $n_0 - 1$  value by 19% and increases  $n_{0,\text{cal}} - 1$  by 21%. Therefore, if the waist radius were calibrated for partial alignment, the  $n_0 - 1$  and  $n_{0,\text{cal}} - 1$  values could become closer.

The temporal signals of laser pulses measured by a photodiode and theoretical calculation on the Ar-seeded molecular beam<sup>17</sup> give the laser pulse width  $\tau = 7 \text{ ns}$  and the molecular beam velocity  $v_0 = 580 \text{ m/s}$ , respectively. By inserting these parameters into Eq. (15) we get the SELFOC slab thickness of  $4.2 \mu\text{m}$ . Note that the velocities of different molecules in the same molecular beam with argon buffer gas are equal and the thickness of the equivalent SELFOC slab is the same for both benzene and nitric oxide. However, they have different focal lengths due to their different molecule-optical refractive indices. The focal lengths for benzene and nitric oxide molecular beams calculated from Eq. (14) are 0.22 and 0.75 mm, respectively. This focal length difference can be understood as chromatic aberration in molecule optics.

The portion near  $y = \pm w_0/2$  of this SELFOC slab can be used as a separation tool, molecule prism. After the mixture molecular beam of benzene and nitric oxide passes through the molecule prism, the two molecular species are refracted or deflected in different directions according to their molecule-optical refractive index values. Figure 3 shows the spatial separation of benzene and nitric oxide neutral molecules at the position of  $v_0 \times \text{TOF}$  which has been converted from the images of molecular ions accelerated by the focusing electrodes. The left image is for benzene molecules with the deflecting laser turned off. After calibrating the difference in ion signal intensities from a given laser pulse and the artifacts of imperfect focusing electrodes, the right image depicts the separation of benzene and nitric oxide molecules in  $25.9 \mu\text{s}$  after the deflecting laser turned on. At  $y = w_0/2$ , the molecule prism shifts the rays of molecules downward

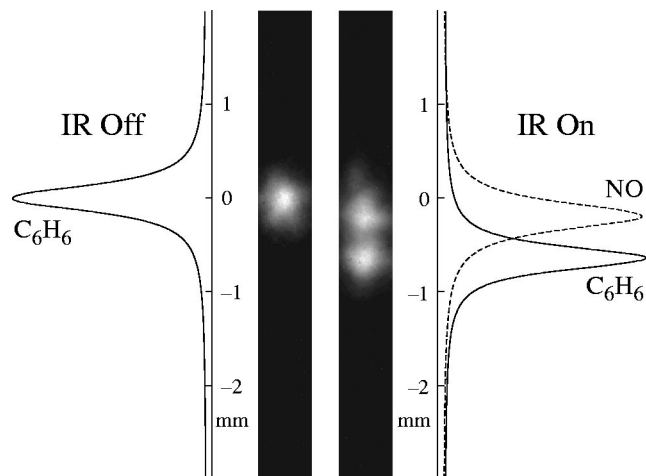


FIG. 3. The spatial separation of benzene and nitric oxide neutral molecules at the position of  $v_0 \times \text{TOF}$ . The IR laser is circularly polarized with peak intensity  $I_0 = 2.7 \times 10^{12} \text{ W/cm}^2$ . The left image is for benzene molecules with the deflecting laser turned off. The right image depicts the separation of benzene and nitric oxide molecules with the deflecting laser turned on. Intensities of the images for benzene (solid line) and nitric oxide (dotted line) integrated over the band are plotted on the side.

and the benzene molecules with a larger  $n$  are more deflected than the nitric oxide molecules with a smaller value of  $n$ . The chromatographic resolution<sup>18</sup> of 0.62 between the two peaks is obtained with the molecule prism formed by a circularly polarized pulse of  $2.7 \times 10^{12} \text{ W/cm}^2$ . In addition to the initial transverse velocity spread before the ionization, the ionization detection causes various sources of blurring, which are residual photon energy over ionization energy, repulsion between ions, cross talk between individual pores of the MCP, and spreading of amplified electrons in the gap between the MCP and the phosphor screen. From a simple line-of-sight argument the initial transverse velocity spread  $D_N v_0 / l$  is 3.4 m/s with the nozzle diameter  $D_N = 0.5 \text{ mm}$  and the distance from the nozzle to the dye laser focus  $l = 85 \text{ mm}$ . Ionization energies of benzene and nitric oxide are 9.24 and 9.26 eV, respectively. Benzene ions acquired a velocity change  $\sim 2.7 \text{ m/s}$  from the residual energy of six 644.1 nm photons. That for nitric oxide is less than 2.9 m/s since the (3+2) REMPI process ionizes nitric oxide into a  $v^+ = 1$  vibrational state,<sup>14</sup> which has about 0.295 eV more energy than the vibrational ground state of  $\text{NO}^+$ .<sup>19</sup> To minimize the ion-ion repulsion, the ionizing dye laser intensity is reduced until the ion image sizes reach a minimum. The blurring due to the detector gave a velocity spread of 3.1 m/s, which was estimated in our previous work by measuring the smallest ion image sizes.<sup>11</sup> These velocity spreads give a total velocity spread of 5.3 m/s for benzene and 5.4 m/s for nitric oxide. Without the instrumental spreads, the resolution of the two neutral species would have been as large as 0.97.

## V. CONCLUSIONS

The interaction of a molecular beam with an intense nonresonant laser field due to a focused nonresonant Nd:YAG laser pulse is viewed as a molecular matter wave passing through a molecule-optical SELFOC slab with a molecule-optical refractive index,  $n$ . Since  $n$  depends on the

molecular properties such as the mass and polarizability as well as the laser field parameters, a molecular matter wave consisting of multiple molecular species can be separated spatially using the portion of a SELFOC slab with maximum dispersion as a molecule prism. A mixture beam of benzene and nitric oxide was thus successfully separated, with a chromatographic resolution of 0.62. The realization of a molecule prism demonstrates the feasibility of molecule optics. In addition, light-based molecule-optical components can provide a new means of manipulating molecules; for example, isomers of identical mass could be separated via the difference in their molecular polarizabilities by combining a conventional mass spectrometer with a molecule prism.

## ACKNOWLEDGMENTS

This work was supported by the KRF (305-20012006) and BK21, Korea. B.F. thanks the U.S. Department of Energy for financial support.

- <sup>1</sup>J. E. Bjorkholm, R. R. Freeman, A. Ashkin, and D. B. Pearson, *Phys. Rev. Lett.* **41**, 1361 (1978).  
<sup>2</sup>E. M. Rasel, M. K. Oberthaler, H. Batelanan, J. Schmiedmayer, and A. Zeilinger, *Phys. Rev. Lett.* **75**, 2633 (1995).  
<sup>3</sup>B. Segev, R. Cote, and M. G. Raizen, *Phys. Rev. A* **56**, R3350 (1997).  
<sup>4</sup>W. Demtroder, *Laser Spectroscopy: Basic Concepts and Instrumentation* (Springer-Verlag, New York, 1996).

- <sup>5</sup>B. Friedrich and D. Herschbach, *Phys. Rev. Lett.* **74**, 4623 (1995); T. Seideman, *J. Chem. Phys.* **107**, 10420 (1997); **106**, 2881 (1997); **111**, 4397 (1999); B. Friedrich and D. Herschbach, *J. Phys. Chem. A* **103**, 10280 (1999); J. Karczmarek, J. Wright, P. Corkum, and M. Ivanov, *Phys. Rev. Lett.* **82**, 3420 (1999).  
<sup>6</sup>H. Stapelfeldt, H. Sakai, E. Constant, and P. B. Corkum, *Phys. Rev. Lett.* **79**, 2787 (1997).  
<sup>7</sup>H. Sakai, C. P. Safvan, J. J. Larsen, K. M. Hilligsoe, K. Hald, and H. Stapelfeldt, *J. Chem. Phys.* **110**, 10235 (1999).  
<sup>8</sup>D. M. Villeneuve, S. A. Aseyev, P. Dietrich, M. Spanner, M. Y. Ivanov, and P. B. Corkum, *Phys. Rev. Lett.* **85**, 542 (2000).  
<sup>9</sup>O. Nairz, B. Brezger, M. Arndt, and A. Zeilinger, *Phys. Rev. Lett.* **87**, 160401 (2001).  
<sup>10</sup>B. S. Zhao, H. S. Chung, K. Cho *et al.*, *Phys. Rev. Lett.* **85**, 2705 (2000).  
<sup>11</sup>H. S. Chung, B. S. Zhao, S. H. Lee, S. Hwang, K. Cho, S.-H. Shim, S.-M. Lim, W. K. Kang, and D. S. Chung, *J. Chem. Phys.* **114**, 8293 (2001).  
<sup>12</sup>C. S. Adams, M. Sigel, and J. Mlynek, *Phys. Rep.* **240**, 143 (1994).  
<sup>13</sup>B. E. A. Saleh and M. C. Teich, *Fundamentals of Photonics* (Wiley, New York, 1991).  
<sup>14</sup>H. S. Carman and R. N. Compton, *J. Chem. Phys.* **90**, 1307 (1989).  
<sup>15</sup>A. Eppink and D. H. Parker, *Rev. Sci. Instrum.* **68**, 3477 (1997).  
<sup>16</sup>K. J. Miller, *J. Am. Chem. Soc.* **112**, 8543 (1990).  
<sup>17</sup>D. R. Miller, in *Atomic and Molecular Beam Methods*, edited by G. Scoles (Oxford University Press, New York, 1988), Vol. 1, p. 17.  
<sup>18</sup>D. C. Harris, *Quantitative Chemical Analysis*, 4th ed. (Freeman, New York, 1995).  
<sup>19</sup>B. Herzberg, *Molecular Spectra and Molecular Structure; IV. Constant of Diatomic Molecules* (Van Nostrand Reinhold, New York, 1966).